RSC Advances

ROYAL SOCIETY OF CHEMISTRY

PAPER

View Article Online
View Journal | View Issue

Cite this: *RSC Adv.*, 2022, **12**, 743

Electrochemical sensor based on screen printed carbon electrode–zinc oxide nano particles/molecularly imprinted-polymer (SPCE–ZnONPs/MIP) for detection of sodium dodecyl sulfate (SDS)

Putri Faradilla,[a] Henry Setiyanto,*[ab] Robeth Viktoria Manurung *[c] and Vienna Saraswaty[d]

The foremost objective of this work is to prepare a novel electrochemical sensor-based screen-printed carbon electrode made of zinc oxide nanoparticles/molecularly imprinted polymer (SPCE–ZnONPs/MIP) and investigate its characteristics to detect sodium dodecyl sulfate (SDS). The MIP that is polyglutamic acid (PGA) film was synthesized *via in situ* electro-polymerization. The SDS's recognition site was left on the surface of the PGA film after extraction using the cyclic voltammetry (CV) technique, facilitating the specific detection of SDS. Moreover, the ZnONPs (~71 nm, polydispersity index of 0.138) were synthesized and effectively combined with the MIP by a drop-casting method, enhancing the current response. The surface of the prepared SPCE–ZnONPs/MIP was characterized by scanning electron microscopy and energy dispersive X-ray. Besides, the electrochemical performance of the SPCE–ZnONPs/MIP was also studied through CV and differential pulse voltammetry (DPV) techniques. As an outstanding result, it is observed that the current response of SPCE–ZnONPs/MIP for detection of SDS remarkably increased almost four times higher from 0.009 mA to 0.041 mA in comparison with bare SPCE. More importantly, the proposed SPCE–ZnONPs/MIP exhibited an excellent selectivity (in the presence of interfering molecules of Ca^{2+}, Pb^{2+}, as well as sodium dodecylbenzene sulfonate (SDBS)), sensitivity, reproducibility, and repeatability. Since the modified sensor offers portability, it is suitable for *in situ* environment and cosmetic monitoring.

Received 13th September 2021
Accepted 29th November 2021

DOI: 10.1039/d1ra06862h

rsc.li/rsc-advances

1. Introduction

Sodium dodecyl sulfate (SDS), an anionic surfactant, also called sodium lauryl sulfate (SLS), is one of the most frequently used additives in household and personal care products (cosmetics).[1] In the household industry, SDS is used as a softener and cleaning agent. Whereas in personal care products, SDS is used as a flocculating or a decolorizing agent. It is imperative to note that SDS concentrations in household products were found at 1–30% w/v. Whereas in several personal care products, SDS was detected at 0.01 to 50% w/v.[2] According to Bondi *et al.* SDS at 0.5–10% w/v causes skin and eye irritation.

Additionally, applying SDS at a concentration higher than 10% w/v in personal care products resulted in dermatitis, including swelling, blistering, or redness.[3] The environmental safety assessment of SDS has shown its toxic potential to the aquatic organisms, particularly on fish fertilization and on the kidney and spleen function. More importantly, SDS is also reported to result in cell damage, a decrease in cell proliferation, and hyperplasia.[4] Additionally, the government Republic of Indonesia has released regulation no. 22/(2021), which mentioned that the allowed concentration of SDS in wastewater (refer to the detergent concentration) is below 0.2 mg L^{-1}.[5] Then, following the cosmetic ingredient review, SDS is potentially harmful. Thus, the preparation of SDS in cosmetics is limited to a maximum concentration of 1%.[6] Therefore, it is essential to evaluate the presence of SDS both qualitative and quantitatively, either in wastewater or personal care products.

Several analytical methods have been used to evaluate SDS, including colorimetry,[7] UV-vis spectrometry,[8] gas chromatography-mass spectrometry,[9] fluorescent,[10] amperometry,[11] potentiometric,[12,13] and voltammetric.[14,15] Those methods are capable of assessing SDS. However, they generate inconvenience, are time-

[a]*Analytical Chemistry Research Group, Institut Teknologi Bandung, Bandung, Indonesia. E-mail: henry@chem.itb.ac.id*

[b]*Center for Defence and Security Research, Institut Teknologi Bandung, Bandung, Indonesia*

[c]*Research Centre for Electronics and Telecommunication, National Research and Innovation Agency Republic of Indonesia, Bandung, Indonesia. E-mail: robeth.viktoria.manurung@lipi.go.id*

[d]*Research Unit for Clean Technology, National Research and Innovation Agency Republic of Indonesia, Bandung, Indonesia*

consuming, expensive, and require complex preparation. Hence, it is urgent to develop an effective, rapid, and simple method for SDS determination. In addition, for environmental monitoring, a portable sensor is preferred.

An electrochemical-based sensor has attracted interest for being developed. An electrochemical-based sensor offers rapid measurement, simple preparation, cost-effectiveness, and portability—undoubtedly, it is very promising. However, a bare working electrode on an electrochemical-based sensor generally only consists of carbon, therefore, exhibits a poor electrochemical response. The performance of an electrochemical-based sensor can be enhanced *via* the electrode materials, for example, by preparing an electrical double-layer sensor, a pseudo sensor, or a hybrid sensor.[16] In this work, we are interested in developing an electrical double layer sensor because it has a more sensitive interfacial property.

Polymers, metal oxide, and carbonaceous materials have been exploited to fabricate an electrical double layer sensor. However, the utilization of pure metal oxide suffers a low conductivity, chemical instability, and mechanical brittleness. Therefore, combining the metal oxide with a binder is better to provide an appropriate composite with a remarkably electrochemical response.[16,17] Among various metal oxides, zinc oxide nanoparticles (ZnONPs) have received interest in electrochemical sensing development because their advantages include environmentally friendly, cheap, high surface area, highly stable material (both physical and chemical), biocompatible and non-toxic. More importantly, ZnONPs have high electrocatalytic activity, accelerating the process evaluation of various analytes.[18–20] Although the ZnO particles have good stability, however, the utilization of ZnONPs is rarely used individually on a modified sensor because of instability issues such as aggregation during the preparation step.[21] Here, several investigators have tried using ZnONPs in combination with other materials such as graphene oxide and multi-walled carbon nanotube, then enhancing the function of the sensors.[20,22]

A molecularly imprinted polymer (MIP) is a polymer containing a functional monomer and a molecule template. It also has reported improving electrochemical-based sensor performance.[23,24] MIP can be easily synthesized either by bulk or *in situ* electro-polymerization.[25] Preparation of MIP by bulk polymerization suffers difficulties in accessing molecules template and low homogeneity. Thus, it requires a more protracted process in removing the molecules template. In reverse, the *in situ* electro-polymerization provides an easier and faster approach to remove the molecule template and generates cavities in uniform shape and size.[24,26–30]

Among various polymers, glutamic acid (GA), a monomer, has been widely used as the functional monomer for MIP-based electrochemical sensing. The poly glutamic acid (PGA) polymer showed a satisfying response in detecting Cd and Pb ions,[31] dopamine,[32] and rhodamine.[33] It seems that the γ-peptide and α-carboxyl groups of PGA play an essential role in selective binding with target analyte *via* electrostatic interaction and covalent bond.[34,35]

In this present work, we modify the SPCE with MIP (PGA) for more excellent selectivity and sensitivity in SDS detection because of its electroactive nature and possibly interacting with PGA *via* hydrogen bond.[23] The MIP was prepared by *in situ* electro-polymerization to provide a facile preparation of the PGA and its molecule template. Later, to improve the electrochemical response and facilitate a better electron transfer, the prepared MIP was further combined with ZnONPs. A set of parameters including optimum conditions for evaluation and the analytical performance of ZnONPs/MIP modified SPCE towards SDS were investigated.

2. Experimental

2.1 Materials

$Zn(CH_3COOH)_2 \cdot 2H_2O$ (99.5–101.0%), KOH (≥85%), L-glutamic acid (99.0–100.5%), sodium dodecyl sulfate (≥99%), sodium hydroxide, KCl (≥99.5%), sodium dodecylbenzene sulfonate, $Pb(NO_3)_2$, $CaCO_3$, $K_3[Fe(CN)_6]$, $K_4[Fe(CN)_6]$, KH_2PO_4 (≥99.995%), and K_2HPO_4 (≥99.99%) are from Merck (Germany) with pro analytical grade. Ultrapure water was prepared by a Module E-pure D4642-33 instrument (Barnstead) with a resistivity ≥18 MΩ. Silver paste and insulator paste (polysiloxane, silicone thickened oil) were purchased from Shoei.

2.2 Apparatus and electrochemical measurement

Particle size analysis was performed using a Zetasizer Nano Series, Malvern (UK). For absorbance measurement, an UV-visible spectrophotometer (Agilent Technologies-8453, Germany) was used. Scanning electron microscopy (SEM) (JEOL

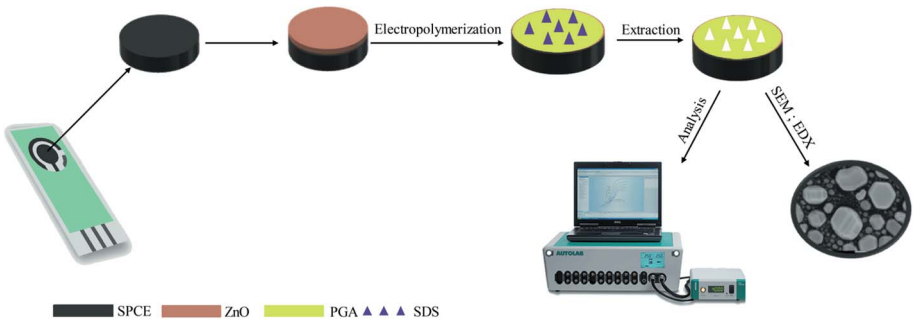

Fig. 1 The schematic diagram of preparation SPCE–ZnONPs/MIP.

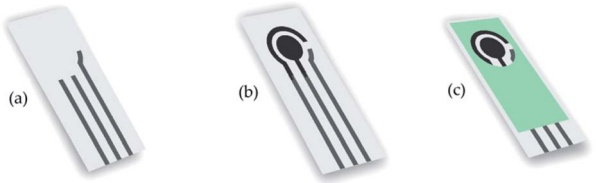

Fig. 2 Step of SPCE fabrication of (a) reference electrode; (b) working, counter electrode; and (c) encapsulation.

JSM IT300, Japan) was used to evaluate the surface morphology of the electrode. In comparison, an energy-dispersive X-ray diffractive (EDX) (Oxford X-Max 20, UK) evaluation was applied to identify the element present on the electrode surface. The electrochemical measurement was recorded using Autolab PGSTAT302N Metrohm. All measurements were performed at room temperature. The surface of SPCE was activated in 0.1 M NaOH using CV technique within the potential range between

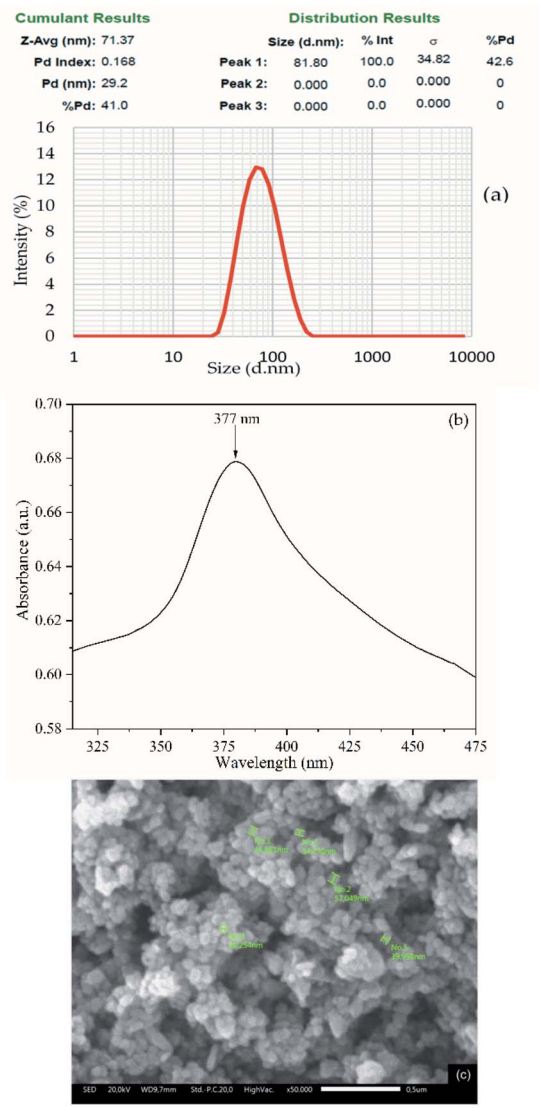

Fig. 3 The (a) particle size distribution and (b) the UV-visible spectra. And (c) SEM image of ZnONPs at 50 000× magnification.

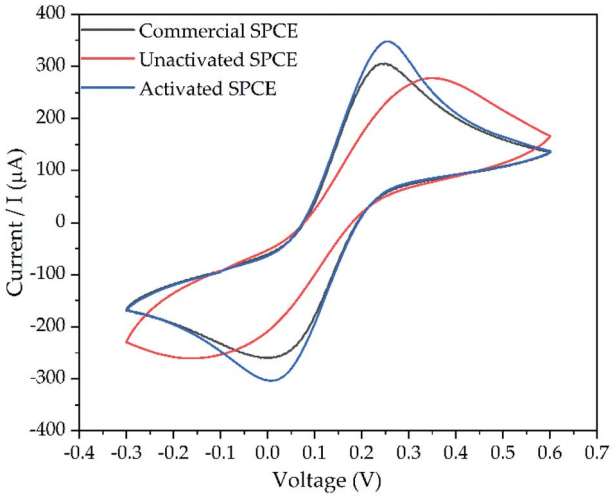

Fig. 4 The CV voltammogram of unactivated SPCE (red line), activated SPCE (blue line), and commercial SPCE (black line).

0 to 1.2 V. CV characterization was performed with 0.01 M $[Fe(CN)6]^{3-/4-}$ in 0.1 M KCl over the potential range −0.3 to 0.6 V with a scan rate of 100 mV s^{-1}. The current of SDS was

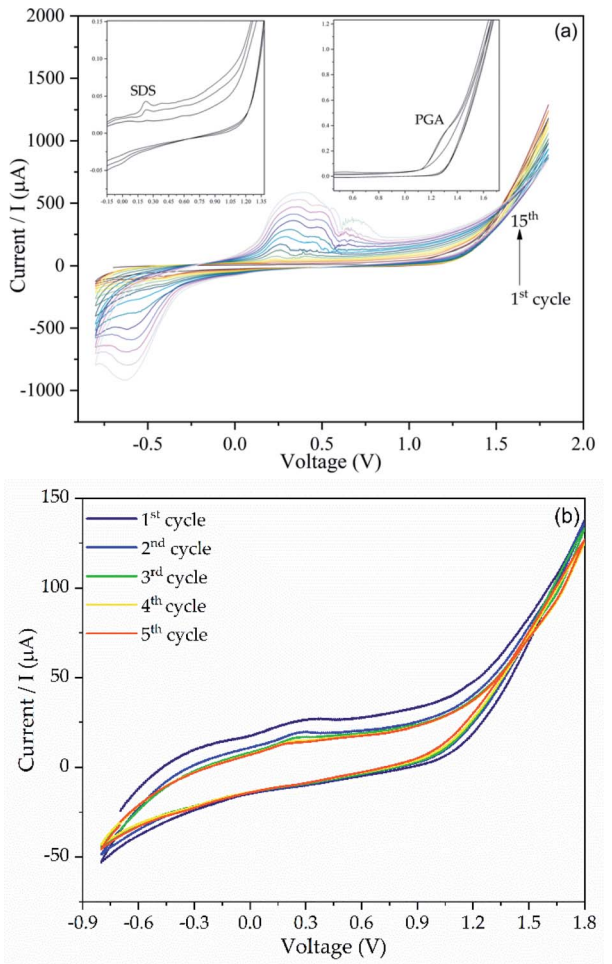

Fig. 5 (a) The CV voltammogram of GA electro-polymerization and (b) extraction process of SDS from the PGA matrix.

measured using DPV at the potential ranging of −0.2 to 0.4 V, and 0.1 M PBS pH 7 was employed as a supporting electrolyte.

2.3 Screen-printed carbon electrode fabrication

The schematic diagram for the fabrication of screen-printed carbon electrodes (SPCE) is illustrated in Fig. 1. As shown, the electrodes were deposited onto an alumina substrate surface (10 mm × 25 mm). The reference electrode was printed using silver paste (Fig. 2a) and dried in the oven. The substrate was then calcinated at 750 °C using a furnace. The working and counter electrodes were printed using carbon paste onto the substrate and dried in an oven at 110 °C (Fig. 2b).

Further, an insulator paste was printed for the encapsulation layer (Fig. 2c). The silver electrode was modified using the electroplating technique in KCl 0.1 M with Pt wire to form a silver/silver chloride electrode. Finally, the surface of SPCE was activated using 50 μL of 0.1 M NaOH to remove the impurities during the fabrication process.

2.4 Preparation of ZnO nanoparticles (ZnONPs)

The ZnONPs were synthesized following the previous work.[36] In separated flasks, about 200 mL of 0.1 M of $Zn(CH_3COOH)_2 \cdot 2H_2O$ and 200 mL of 0.4 M KOH were dissolved in ethanol. Both solutions were heated at 60 °C with constant stirring until completely dissolved. Subsequently, KOH solution was dripped slowly into $Zn(CH_3COOH)_2 \cdot 2H_2O$ solution and continuously stirred for 3 hours. The zinc oxide particles were obtained as a white precipitate. The ZnO particles were then collected by centrifugation at 4000 rpm. Subsequently, the ZnO particles were washed with acetone and ultrapure water to remove the impurities and heated at 600 °C to form ZnONPs (2.2 grams). For optimization, the concentration of ZnONPs suspensions were varied from 0.25 to 1.25 mg mL^{-1}. The ZnONPs suspensions were prepared by dispersing the ZnONPs in ethanol and sonicated for 30 minutes. Later about 2.5 μL of ZnONPs suspension was drop cast onto the surface of the SPCE and was dried at 60 °C.

2.5 Fabrication of SPCE–ZnONPs/MIP

The schematic diagram for the preparation of SPCE–ZnONPs/MIP is presented in Fig. 1. The MIP was prepared by *in situ* electro-polymerization using glutamic acid (GA) as the functional monomer. About 50 μL of the 1 mM GA and 1 mM SDS (1 : 1) mixture in 0.1 M PBS (pH = 7) was dropped onto the SPCE surface for the electro-polymerization process. Subsequently, the *in situ* electro-polymerization of GA was performed using the CV technique at the potential ranging from −0.8 to 1.8 V. Then, the SDS was removed by extraction using ultrapure water, leaving a molecule template on the polymer matrix. For the repeatability measurement, an SPCE–ZnONPs/MIP was used for

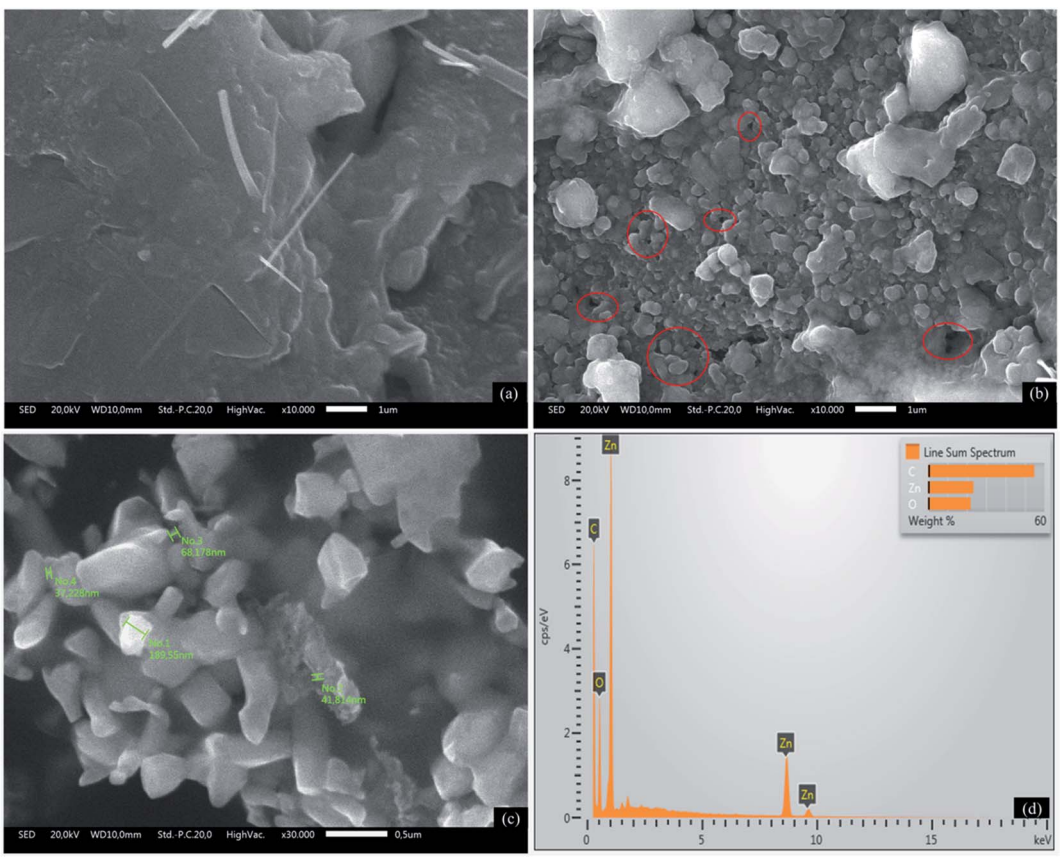

Fig. 6 The surface morphology of: (a) bare SPCE (at 10 000× magnification); (b) SPCE–ZnO/MIP (at 10 000× magnification); (c) SPCE–ZnO/MIP (at 30 000× magnification) and (d) EDX spectrum of SPCE–ZnONPs/MIP.

ten repetitive measurements. The SPCE–ZnONPs/MIP was washed by ultrapure water using the CV technique at the potential range from −0.8 to +1.8 V before repetitive measurement. A non-imprinted polymer (NIP) (SPCE–NIP) was also fabricated for comparing the performance with SPCE–ZnONPs/MIP. The SPCE–NIP was prepared with a similar procedure according to SPCE–MIP preparation without a molecule template.

2.6 Real sample analysis

The laundry wastewater and shampoo were used for the evaluation of SDS in the actual sample. The laundry wastewater (sample 1) was collected from a public place. The laundry wastewater was diluted 100 times using 0.1 M PBS (pH = 7) and directly analyzed using the DPV method. Shampoo (sample 2) was purchased from the supermarket. About 1.0 g of shampoo sample was dissolved in 10 mL of methanol and filtered. The filtrate of shampoo was diluted 100 times using 0.1 M PBS (pH = 7) and analyzed using DPV.

3. Result and discussion

3.1 Synthesis of ZnONPs

The particle size analysis using a PSA showed that the particles of synthesized ZnO, which were synthesized by a wet chemical method, are in nano-size. As depicted in Fig. 3a, the particle size distribution of ZnONPs showed an average diameter size of ~71 nm with a monodisperse system (polydispersity index (PI) = 0.168).[37] The maximum absorption peak of ZnONPs was observed at λ = 377 nm (Fig. 3b), suggesting that the ZnONPs were in the form of hexagonal wurtzite. The SEM image emphasized the formation of nanoparticles of the synthesized ZnONPs (Fig. 3c). As depicted, the SEM image clearly shows that the synthesized ZnONPs are crystalline with a wurtzite structure with particles size below ~100 nm. This is closely related to the results of particle size and maximum absorption peak evaluation.[38–42]

3.2 Cyclic voltammetry (CV) behavior of the fabricated SPCE

The fabricated SPCE should be activated before the characterization. The activation step aimed to remove impurities and enhance the electron transfer. In this work, the fabricated SPCE was activated with 50 μL of 0.1 M NaOH solution. As a comparison, a commercial SPCE was used to investigate the performance of the fabricated SPCE without activation. The CV behavior of commercial SPCE activated SPCE, and unactivated SPCE are shown in Fig. 4. As depicted, the activated SPCE showed a higher peak current (I_{pa} = 0.26 mA, I_{pc} = 0.23 mA, ΔE = 0.21 V) in comparison with unactivated SPCE (I_{pa} = 0.20 mA, I_{pc} = 0.12 mA, ΔE = 0.27 V) as well as commercial SPCE (I_{pa} = 0.22 mA, I_{pc} = 0.19 mA, ΔE = 0.22 V). This is probably due to the removal of covering organic binders on the surface of SPCE. Thus, the functionality and sensitivity of the surface of SPCE as a working electrode improved.[43,44]

3.3 Electropolymerization of glutamic acid (GA) on SPCE–ZnONPs

The SPCE–ZnONPs were modified using GA by *in situ* electropolymerization. The CV responses during *in situ* electropolymerization of GA on the electrode surface can be seen in Fig. 5a. As depicted, the oxidation peak of SDS and GA present at working potential values of 0.18 and 1.2 V, respectively.[45–47] We recorded a successful formation of PGA film by the presence of the oxidation peak at a potential working value of −0.8 to +1.8 V. The oxidation peak at 1.2 V indicated that the amino group from GA was oxidized to a radical cation. Therefore, the polymerization of GA occurred due to interaction between the radical cation with a deprotonated carboxyl group (–COOH–) from other GA molecules.[48] Moreover, the amino group radical cations established carbon-nitrogen linkages on the electrode surface.[47]

After electro-polymerization, the SDS molecules were then extracted from the polymer matrix to create a cavity as an SDS

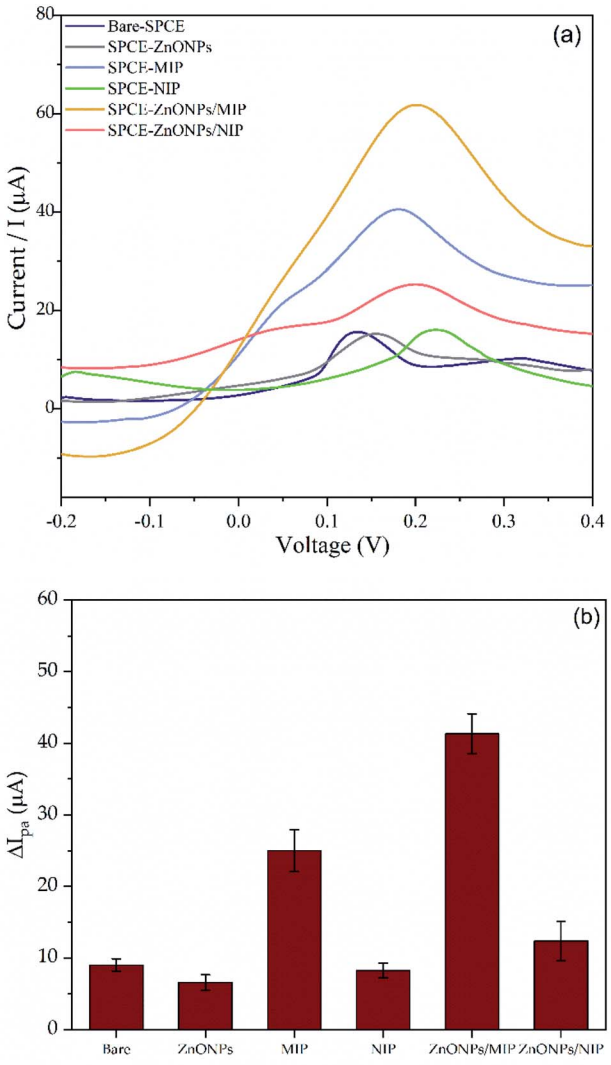

Fig. 7 (a) DPV voltammogram and (b) histogram of SDS oxidation peak.

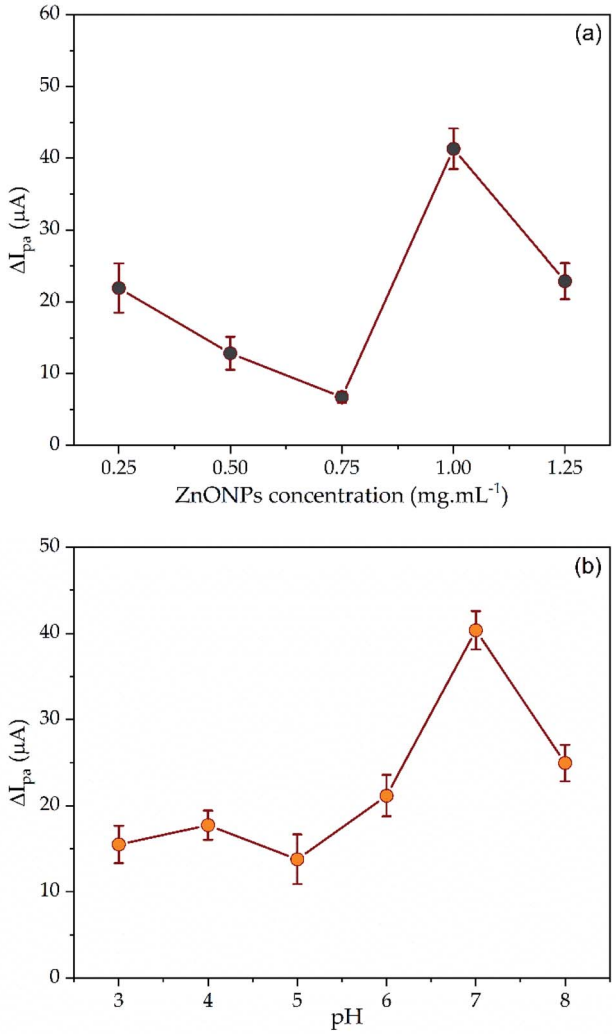

Fig. 8 (a) The influence of ZnONPs concentration and (b) pH on anodic currents of 0.1 mM SDS on the SPCE–ZnONPs/MIP.

site. The CV voltammogram of SPCE–ZnONPs/MIP before and after extraction of SDS from the PGA matrix can be seen in Fig. 5b. As shown, a decrease of oxidation peak at a working potential of 0.18 V was observed on the second cycle (blue line) of extraction, showing that SDS molecules start to be removed from the polymer matrix. The absence of oxidation peak after the 5th extraction cycle, indicating a complete SDS removal.[49]

3.4 Surface morphology and EDX characterization of modified SPCE

SEM observation was applied to study the changes in surface morphology of SPCE–ZnONPs/MIP sensing. The morphology clearly shows that the bare SPCE (Fig. 6a) has a smoother surface than the modified SPCE. The surface of SPCE–ZnONPs/MIP (Fig. 6b) showed a rougher surface, suggesting that the MIP and ZnONPs successfully drop cast on the surface of SPCE. More importantly, as depicted by the red circle in Fig. 6b, the cavities present on the surface of SPCE–ZnONPs/MIP confirmed the successful polymerization of PGA and extraction SDS from the PGA matrix. Further, to verify that the ZnONPs have been drop cast on the SPCE, an EDX evaluation was applied. The EDX image (Fig. 6c) depicted the presence of carbon, oxygen, and Zn element. No doubt, it is confirmed that the ZnONPs successfully drop cast.

3.5 The electrochemical response of SDS on modified SPCE

Electrochemical responses of 0.1 mM SDS on several modified SPCE were observed by differential pulse voltammetry (DPV) in 0.1 M PBS (pH = 7). We use the DPV technique to evaluate SDS response due to its advantage to provide higher current sensitivity, and better resolution than CV.[50,51] Fig. 7 shows the DPV voltammogram and the histogram of SDS electrochemical response. As shown in Fig. 7b, the peak current of SDS responses on SPCE–NIP and SPCE–ZnONPs are similar to the response SDS on the bare SPCE. However, it was observed that the peak current response of SPCE–ZnONPs is lower than the bare SPCE. Factors that influence the electrochemical response are (1) the diffusion of the analyte, (2) the electrochemical catalytic reaction, and (3) the electron transport.[52] Since the ZnONPs were simply dropping cast individually on the surface of SPCE, and therefore when the modified electrode was dried, the ZnONPs tended to agglomerate. Then reducing the peak current response due to the decrease in diffusion of SDS onto the surface of SPCE.[53]

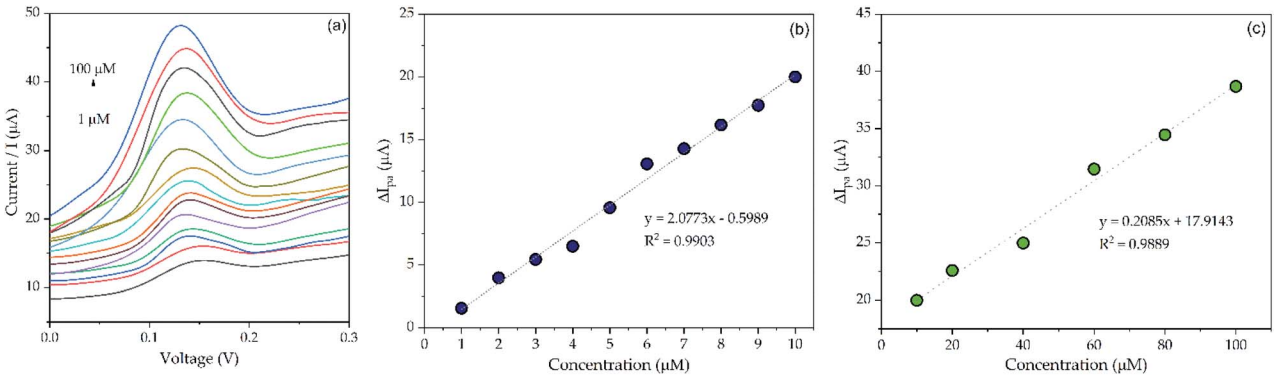

Fig. 9 (a) DPV voltammogram of SDS at 1–100 μM; (b) plot of SDS concentration (1–10 μM) *vs.* anodic peak current; (c) plot of SDS concentration (10–100 μM) *vs.* anodic peak current.

A significant increment of SDS responses were observed on SPCE–MIP, SPCE–ZnONPs/NIP, and SPCE–ZnONPs/MIP with peak current values (Ipa) of 0.025 mA, 0.012 mA, and 0.041 mA, respectively. The SPCE/ZnONPs-NIP exhibited the poorest response as compared with SPCE–MIP and SPCE–ZnONPs/MIP. Conversely, the SPCE–ZnONPs/MIP exhibited the most significant current response. It seems the MIP plays an essential role as an organic binder for ZnONPs, reducing the aggregation of ZnONPs after drop cast on modified SPCE. Therefore, providing a better electrocatalytic activity.[54,55] In addition, the presence of MIP cavities provides a highly selective template for SDS evaluation. No doubt, by combining the MIP with ZnONPs, the performance of the modified electrode remarkably improved.

3.6 Optimization of SPCE–ZnONPs/MIP

3.6.1 Effect of ZnONPs concentration. The influence of ZnONPs concentrations at 0.25; 0.5; 0.75; 1; 1.25 mg mL^{-1} towards the peak current responses of SDS at 0.1 mM on SPCE–ZnONPs/MIP were observed. As shown in Fig. 8a, the highest peak anodic current response at a working potential of 0.18 V was recorded when 1 mg mL^{-1} ZnONPs (0.041 mA) were applied. When the concentration of ZnONPs was increased to 1.25 mg mL^{-1}, a decrease in peak current response was observed. Studies have shown that applying nanoparticles at high concentrations is less effective.[56,57] This is due to the nature of nanoparticles which tend to agglomerate.[58] Therefore, increasing the thickness of the modified layer on the surface working electrode reduces the electron transfer.[59] For this reason, we recommended applying ZnONPs at a concentration below 1.25 mg mL^{-1} on modified SPCE.

3.6.2 The influence of pH. The influence of pH on the electrochemical behavior of 0.1 mM SDS was observed in 0.1 M PBS at pH 3–8 (Fig. 8b). The results showed that the highest anodic peak current was conducted at pH 7. The sulfate end group of SDS will only be protonated at a very low pH.[60,61] Whereas in alkaline conditions (pH > 7), SDS micelles will be highly charged and hardly for being oxidized.[62,63] The phenomenons resulted in a decrease in SDS binding with MIP, thus lowering the I_p value. Undoubtedly, the more SDS filled the cavities of the MIP template in a neutral environment (pH = 7), resulting in the highest current response.

3.7 Performance of the SPCE–ZnONPs/MIP sensing

3.7.1 The linearity. To test the performance of the optimized method, we observed the linear dynamic range of SDS at 1–100 μM using the DPV technique. Fig. 9a showed the voltammogram behavior of SDS. As shown, the peak current response of SDS was observed at a potential value of 0.15–0.18 V. The linear dynamic range of SDS was presented at 1–10 μM with an R^2 value of 0.9903, which relate to regression equation $y = 2.0773x - 0.5989$ (Fig. 9b). A decrease in linearity was noticed at higher concentrations (10–100 μM) (Fig. 9c); this is probably due to the saturation of the recognition site on the electrode surface.[64,65] The limit of detection was calculated according to the linear regression of $y = 2.0773x - 0.5989$. The LOD was

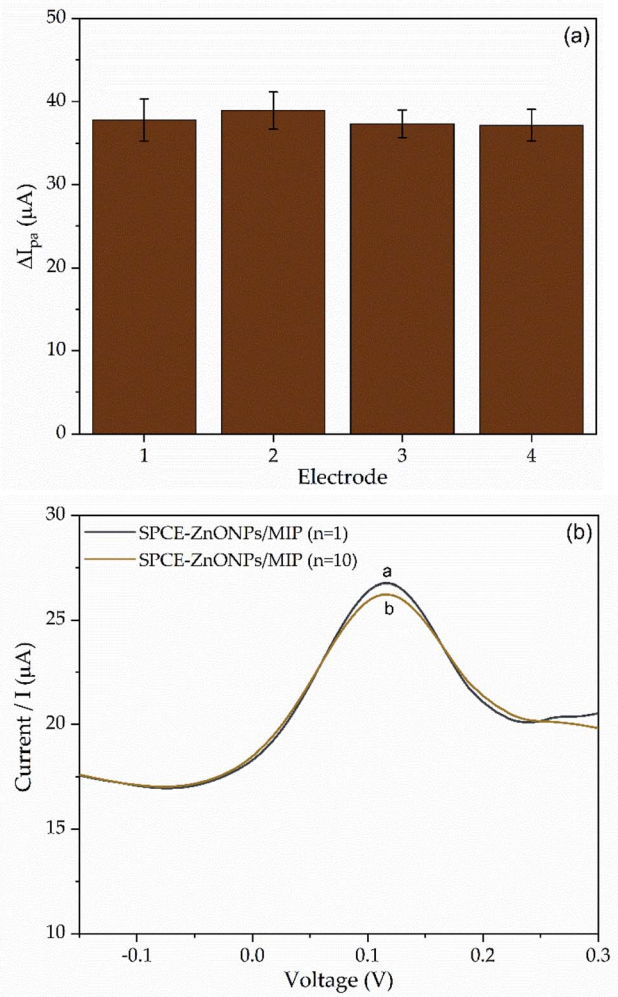

Fig. 10 (a) The peak current of 0.1 mM SDS response on four different SPCE–ZnONPs/MIP and (b) the DPV curve of the repeatability measurement on an SPCE–ZnONPs/MIP.

Table 1 Comparison of linear dynamic range (LDR), LOD, and %RSD of the developed sensor and other methods

Modified electrode	Method	Ref.	LDR	LOD	% RSD
HMDE	AdSV	14	0.05–17.50 μg mL^{-1}	1.2 ng mL^{-1}	2.1%
Eosin Y/polietilenimina	DPV	15	1–40 μg mL^{-1}	0.90 μg mL^{-1}	3.4%
Au-SPE/MIP	DPV	45	0.1–1000 pg mL^{-1}	0.18 pg mL^{-1}	4.9%
ZnO/MIP	DPV	This work	0.2883–2.883 μg mL^{-1}	0.188 μg mL^{-1}	2.1%

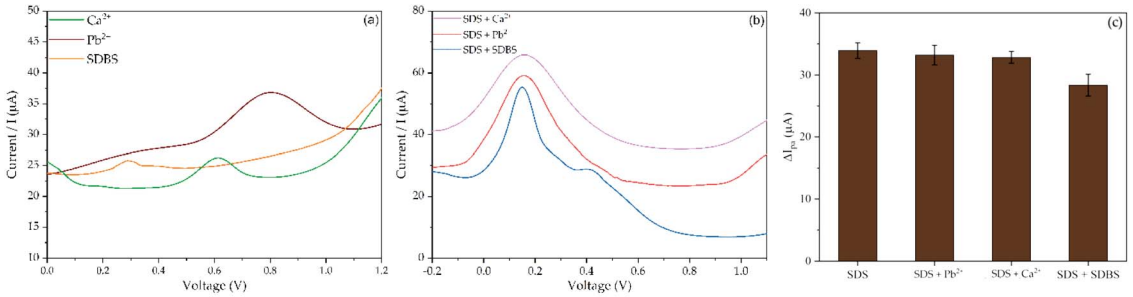

Fig. 11 (a) Voltammogram of 0.1 mM interferent molecules on bare SPCE; (b) 0.1 mM SDS containing interferences (0.1 mM) on SPCE–ZnONPs/MIP; and (c) histogram of oxidation peak current of 0.1 mM SDS solution in the presence of interferences (0.1 mM) on SPCE–ZnONPs/MIP.

determined as "$3\delta a/b$", where 'δa' is the standard error of the intercept, and 'b' is the slope of the calibration curve. The LOD value was found to be 0.652 μM (0.188 μg mL^{-1}). In comparison to other studies[14,15,45] (see Table 1), the linearity of our modified SPCE shows a moderate performance. However, referring to the total amount of detergent allowed, that is, should be below 0.2 mg L^{-1},[5] our modified SPCE can be applied for monitoring of SDS in the environment.

3.7.2 The reproducibility, repeatability, stability, and selectivity of the SPCE–ZnONPs/MIP sensing. For reproducibility evaluation, four repetitive measurements of 0.1 mM SDS were observed ($n = 4$). As depicted in Fig. 10A, it shows that the sensitivity response of the SPCE–ZnONPs/MIP to SDS detection is highly reproducible as suggested by a % relative standard deviation (RSD) of 2.10%. The repeatability and stability of the SPCE–ZnONPs/MIP were also tested for ten repetitions ($n = 10$). The SPCE–ZnONPs/MIP electrode was washed with ultrapure water using the CV technique to remove the analyte from the template before repetition. As illustrated in Fig. 10b, the DPV curve obtained at the newly prepared SPCE–ZnONPs/MIP (curve *a*) and the DPV recorded after ten repetition measurements (curve *b*) were almost the same. The appearance of SPCE–ZnONPs/MIP showed no defect after ten repetitive measurements. These results were emphasized by calculation of the % RSD and %RSD Horwitz of 4.76% and 9.74%, respectively, suggesting that the modified electrode had good repeatability and stability for a short-term evaluation.[15,66] The performance of our modified electrode was similar to an evaluation of SPCE–MIP based sensor, which showed that an SPCE–MIP sensor still exhibits a good performance after ten times repetitive measurements.[15,30]

Further, the selectivity of SPCE–ZnONPs/MIP was tested in the presence of some interfering compounds, including Pb^{2+}, Ca^{2+}, and SDBS. The oxidation peak of those interferents present at the potential value of 0.80 V, 0.61 V, and 0.29 V, respectively (see Fig. 11a) on the bare SPCE. The voltammogram of SDS in the presence of interferents can be seen in Fig. 11b. As depicted, the peaks of interferent molecules were not detected. However, a decrease in peak current response of SDS + SDBS occurred, as shown in Fig. 11c. The structures of SDS and SDBS are similar,[67] thus creating a strong competition between SDS and SDBS molecules to fill the cavities of molecule template on the polymer matrix, then decreasing the peak current response.[12,15] Considering that the changes of peak current response of SDS in the presence of interferents are less than 10% (between 1–9.15%). Those molecules did not cause significant interference.[66]

3.8 Analysis of real samples

Finally, to test that our proposed method is applicable for evaluating real samples, we analyzed SDS concentration in laundry wastewater and shampoo. UV-visible spectrophotometry was used to confirm whether the measurement was accurate or not. As presented in Table 2, both the proposed method and UV-vis spectrophotometry evaluation are in good agreement for SDS determination. This was also emphasized by the calculation of t_{exp} and t_{table}, which show that the t_{exp} is lower than t_{table}, indicating that the proposed method is acceptable.[68] In addition, the percentage recovery (%R) of SDS from the laundry wastewater and shampoo were 97.07 and 94.27% (see Table 3), revealing that our proposed method accurately detects SDS in real samples.[2,66]

The determination of SDS concentration using SPCE–ZnONPs/MIP provides a rapid and straightforward analysis. This is because the amount of samples required for the evaluation is only 50 μL, which is fewer than the evaluation using UV-

Table 2 The comparison of SDS concentration in laundry wastewater and shampoo was evaluated using DPV at SPCE–ZnONPs/MIP and UV-vis spectrometry technique

	DPV	UV-visible		
Sample	Concentration (μM ± % RSD)	Concentration (μM ± % RSD)	t_{exp}	t_{table}
Laundry wastewater	370.6 ± 1.95	342.6 ± 3.02	3.840	4.3
Shampoo	524.7 ± 1.48	522.3 ± 3.07	0.015	4.3

Table 3 The percentage recovery of SDS from laundry wastewater and shampoo

Sample	Concentration (μM)	Spiked (μM)	Measured (μM)	Recovery (%)
Laundry wastewater	3.71	5	8.45	97.07
Shampoo	5.25	5	9.66	94.27

visible spectrophotometry (2 mL). Thus, undoubtedly, our method exhibits an effective analysis with less time and sample consumption.

More importantly, compared to another electrochemical method in SDS evaluation, which uses Au-based screen printing electrode (Au-SPE),45 our proposed sensing is a carbon-based SPE, therefore cheaper than Au-SPE. Although the Au-SPE has shown more sensitive sensor performance, however, considering the low-cost preparation of carbon-based SPE, providing a sensitive electrochemical response, and capable of evaluating the SDS concentration below the stated concentration by government regulation, our modified SPCE are possible to be applied in a large scale, and powerful to be used for monitoring of SDS in wastewater runs off.

4. Conclusions

In summary, an electrochemical sensing-based SPCE–ZnONPs/MIP is developed for the detection of SDS. A simple and effective drop-casting technique is used to prepare the ZnONPs/MIP on the SPCE substrate. Electrochemical studies show that the modified electrode performs well towards the detection of SDS at pH 7. The linear dynamic range of SDS is 1–10 μM with LOD of 0.652 μM (0.188 μg mL^{-1}) at the developed electrode. It is observed that the repeatability performance of the developed electrode is verified as suggested by a similar response after ten repetitive DPV tests. Most interestingly, the current response of SDS is improved up to four times higher by combining the MIP with ZnONPs, suggesting a better electrocatalytic activity. Considering the high % *R* of SDS from the real samples and its portability, the proposed SPCE–ZnONPs/MIP has a promising application for monitoring SDS directly in the environment.

Author contributions

Data collection, data analysis, manuscript writing (PF). Design, concept, data collection, analysis, interpretation, and manuscript writing (HS and VS). Data collection, fabrication, and modification of SPCE, data analysis, and manuscript finalization (RVM).

Conflicts of interest

There is no conflict to declare.

Acknowledgements

This work was funded by P2MI Faculty of Mathematics and Sciences ITB under contract no. 61/IT.1.CO2/SK-TA/2021 and National Research and Innovation Agency (BRIN) under scheme INSINAS grant no. 12/INS/PPK/E4/2021. The authors thank the Department of Chemistry (Analytical Chemistry), Faculty of Mathematics and Natural Sciences, Bandung Institute of Technology, Research Centre for Electronics and Telecommunication and Research Unit for Clean Technology – National Research and Innovation Agency Republic of Indonesia for supporting this work. The authors also acknowledge the facilities, scientific and technical support from Advanced Characterization Laboratories Bandung, National Research and Innovation Agency Republic of Indonesia through e-Layanan Sains.

References

1 W. Fu, F. Qu, G. Yu and J. You, *Sens. Actuators, B*, 2017, **245**, 774–779.
2 C. A. Bondi, J. L. Marks, L. B. Wroblewski, H. S. Raatikainen, S. R. Lenox and K. E. Gebhardt, *Environ. Health Insights*, 2015, **9**, 27–32.
3 S. Kumar, T. J. Kirha and T. Thonger, *J. Chem. Pharm. Res.*, 2014, **6**(5), 1488–1492.
4 L. Ooi, L. Y. Heng and A. Ahmad, *J. Sens.*, 2014, **2015**, 809065.
5 The Government Regulation of the Republic of Indonesia Number 20, Implementation of Environmental Protection and Management, 2021.
6 U. S. Food and Drug Administration, *Food and Drug Administration Department of Health and Human Services*, 2021, vol. 3.
7 X. Chen, S. Kang, M. J. Kim, J. Kim, Y. S. Kim, H. Kim, B. Chi, S. Kim, J. Y. Lee and J. Yoon, *Angew. Chem., Int. Ed. Engl.*, 2010, **49**(8), 1422–1425.
8 E. Rodenas-Torralaba, B. F. Reis, A. Morales-Rubio and M. d. l. Guardia, *Talanta*, 2005, **66**, 591–599.
9 N. Shende, A. Karale, P. Marathe, S. Chakraborty, A. D. Mallya and R. M. Dhere, *Biologicals*, 2019, **60**, 68–74.
10 C. L. Zheng, Z. X. Ji, J. Zhang and S. N. Ding, *Analyst*, 2014, **139**, 3476–3480.
11 A. N. Reshetilova, I. N. Semenchukb, P. V. Iliasov and L. A. Taranovab, *Anal. Chim. Acta*, 1997, **347**, 19–26.
12 T. A. Ali and G. G. Mohamed, *J. AOAC Int.*, 2015, **98**, 116–123.
13 N. M. Makarova and E. G. Kulapina, *Russ. J. Electrochem.*, 2015, **51**, 672–678.
14 A. R. Ghiasvand, Z. Taherimaslak and M. Allahyari, *Int. J. Electrochem. Sci.*, 2009, **4**, 320–335.
15 X. Hao, J. L. Lei, N. B. Li and H. Q. Luo, *Anal. Chim. Acta*, 2014, **852**, 63–68.
16 R. Eivazzadeh-Keihan, R. Taheri-Ledari, M. S. Mehrabad, S. Dalvand, H. Sohrabi, A. Maleki, S. M. Mousavi-Khoshdel and A. E. Shalan, *Energy Fuels*, 2021, **35**, 10869–10877.

17 M. F. Sanad, V. S. N. Chava, A. E. Shalan, L. G. Enriquez, T. Zheng, S. Pilla and S. T. Sreenivasan, *ACS Appl. Mater. Interfaces*, 2021, **13**(34), 40731–40741.
18 T. Sen, S. Mishra, S. S. Sonawane and N. G. Shimpi, *Polym. Eng. Sci.*, 2018, **58**, 1438–1445.
19 M. R. Ganjali, F. G. Nejad and H. Beitollahi, *Int. J. Electrochem. Sci.*, 2017, **12**, 3231–3240.
20 T. Gan, A. Zhao, S. Wang, Z. Lv and J. Sun, *Sens. Actuators, B*, 2016, **235**, 707–716.
21 Z. Wang, H. Li, F. Tang, J. Ma and X. Zhou, *Nanoscale Res. Lett.*, 2018, **13**, 202.
22 T. Kokab, A. Shah, M. A. Khan, M. Arshad, J. Nisar, M. N. Ashiq and M. A. Zia, *ACS Appl. Nano Mater.*, 2021, **4**(5), 4699–4712.
23 R. Gui, H. Jin, H. Guo and Z. Wang, *Biosens. Bioelectron.*, 2018, **100**, 56–70.
24 T. Gan, J. Li, A. Zhao, J. Xu, D. Zheng, H. Wang and Y. Liu, *Food Chem.*, 2018, **268**, 1–8.
25 A. Chiappini, L. Pasquardin and A. M. Bossi, *Sensors*, 2020, **20**, 5069.
26 T. Gan, J. Li, L. Xu, S. Guo, A. Zhao and J. Sun, *Microchim. Acta*, 2020, **187**, 291.
27 A. Yarman and F. Scheller, *Sensors*, 2020, **20**, 2677.
28 L. M. Gonçalves, *Curr. Opin. Electrochem.*, 2021, **25**, 100640.
29 T. Kitto, C. B. Guen, N. Rossetti, and F. Cicoira, Processing and patterning of conducting polymers for flexible, stretchable, and biomedical electronics, in *Handbook of Organic Materials for Electronic and Photonic Device, Woodhead Publishing Series in Electronic and Optical Materials*, 2nd edn, 2019, pp. 817–842.
30 D. Dechtrirat, B. Sookcharoenpinyo, P. Prajongtat, C. Sriprachuabwong, A. Sanguankiat, A. Tuantranont and S. Hannongbua, *RSC Adv.*, 2018, **8**, 206.
31 S. L. Wei, L. Yan, X. Huang, J. Li, S. Yao, H. Zhang and A. Xu, *Ionics*, 2021, **27**, 375–387.
32 M. N. Bui, C. A. Li and G. H. Seong, *BioChip J.*, 2012, **6**, 149–156.
33 H. Setiyanto, F. Ferizal, V. Saraswaty, R. S. Rahayu and M. A. Zulfikar, *IOP Conf. Ser.: Mater. Sci. Eng.*, 2021, **1088**, 012113.
34 Y. Lin, K. Liu, C. Liu, L. Yin, Q. Kang, L. Li and B. Li, *Electrochim. Acta*, 2014, **133**, 492–500.
35 J. J. Feminus, R. Manikandan, S. S. Narayanan and P. N. Deepa, *J. Chem. Sci.*, 2019, **131**, 11.
36 N. M. Shamhari, B. S. Wee, S. F. Chin and K. Y. Kok, *Acta Chim. Slov.*, 2018, **65**, 578–585.
37 N. Akbar, Z. Aslam, R. Siddiqui, M. R. Shah and N. A. Khan, *AMB Express*, 2021, **11**, 104.
38 M. Pudukudy and Z. Yaakob, *J. Cluster Sci.*, 2014, **26**, 1187–1201.
39 D. Jain, Shivani, A. A. Bhojiya, H. Singh, H. K. Daima, M. Singh, S. R. Mohanty, B. J. Stephen and A. Singh, *Front. Chem.*, 2020, **8**, 778.
40 Z. M. Al-Asady, A. H. AL-Hamdani and M. A. Hussein, *AIP Conf. Proc.*, 2020, **2213**, 020061.
41 A. B. Lavand and Y. S. Malghe, *Int. J. Photochem.*, 2015, 305–310.
42 U. S. Rao, G. Srinivas and T. P. Rao, *Procedia Mater. Sci.*, 2015, **10**, 90–96.
43 S. Palanisamy, C. Karuppiah, S. Chen and P. Periakaruppan, *Electroanalysis*, 2014, **26**, 1984–1993.
44 R. A. D. Faria, Y. Messaddeq, L. G. D. Heneine and T. Matencio, *Int. J. Biosens. Bioelectron.*, 2019, **5**(1), 1–2.
45 S. Motia, I. A. Tudor, L. M. Popescu, R. M. Piticescu, B. Bouchikhi and N. El Bari, *J. Electroanal. Chem.*, 2018, **823**, 553–562.
46 D. P. Santos, M. V. B. Zanoni, M. F. B. Bergamini, A. Chiorcea-Paquim, V. C. Diculescu and A. O. Brett, *Electrochim. Acta*, 2008, **53**, 3991–4000.
47 L. Zhang and X. Lin, *Analyst*, 2001, **126**, 367–370.
48 S. Pruneanu, F. Pogacean, C. Grosan, E. M. Pica, L. V. Bolundut and A. S. Biris, *Chem. Phys. Lett.*, 2011, **504**, 56–61.
49 I. Seguro, J. G. Pacheco and C. Delerue-Matos, *Sensors*, 2021, **21**, 1975.
50 M. Amare and S. Admassie, *Bull. Chem. Soc. Ethiop.*, 2012, **26**, 73–84.
51 Y. Zhou, W. Tang, J. Wang, G. Zhang, S. Chai, L. Zhang and T. Liu, *Anal. Methods*, 2014, **6**, 3474.
52 Y. Li, P. Kang, H. Huang, Z. Liu, G. Li, Z. Guo and X. Huang, *Sens. Actuators, B*, 2020, **307**, 127639.
53 D. Antuña-Jiménez, M. B. González-García, D. Hernández-Santos and P. Fanjul-Bolado, *Biosensors*, 2020, **10**, 9.
54 L. Nemcek, M. Šebesta, M. Urík, M. Bujdoš, E. Dobročka and I. Vávra, *Plants*, 2020, **9**, 1365.
55 S. Chaudhary, A. Umar, K. K. Bhasin and S. Baskoutas, *Materials*, 2018, **11**, 287.
56 D. Martín-Yerga, D. Bouzas-Ramos, M. Menéndez-Miranda, A. R. M. Bustos, J. R. Encinar, J. M. Costa-Fernández, A. Sanz-Medel and A. Costa-García, *Electrochim. Acta*, 2015, **166**, 100–106.
57 J. Gross, S. Sayle, A. R. Karow, U. Bakowsky and P. Garidel, *Eur. J. Pharm. Biopharm.*, 2016, **104**, 30–41.
58 M. A. Ashraf, W. Peng, Y. Zare and K. Y. Rhee, *Nanoscale Res. Lett.*, 2018, **13**, 214.
59 L. Ozcan and Y. Sahin, *Sens. Actuators, B*, 2007, **127**, 362–369.
60 D. R. Albano and F. Sevilla III., *Sens. Actuators, B*, 2007, **121**, 129–134.
61 N. Alizadeh and M. Mahmodian, *Elecctroanalysis*, 2000, **12**, 7.
62 G. A. E. Mostafa, *Int. J. Environ. Anal. Chem.*, 2008, **88**, 435–446.
63 C. Trellu, N. Oturan, Y. Pechaud, E. D. van Hullebusch, G. Esposito and M. A. Oturan, *Water Res.*, 2017, **118**, 1–11.
64 M. Ghalkhani, F. Ghelichkhani and F. Ghorbani-Bidkorbeh, *Iran. J. Pharm. Res.*, 2018, **17**, 44–53.
65 W. Argoubi, M. Saadaoui, S. B. Aoun and N. Raouafi, *Beilstein J. Nanotechnol.*, 2015, **6**, 1840–1852.
66 S. F. Beckert and W. S. Paim, *Int. J. Metrol. Qual. Eng.*, 2017, **8**, 23.
67 A. K. Anas, S. Y. Pratama, A. l Izzah and M. A. Kurniawan, *Bull. Chem. React. Eng. Catal.*, 2021, **16**, 188–195.
68 T. K. Kim, *Korean J. Anesthesiol.*, 2015, **68**, 540–546.